

# Efficient high-power diode-end-pumped TEM<sub>00</sub> Nd:YVO<sub>4</sub> laser with a planar cavity

Yung-Fu Chen

Department of Electrophysics, National Chiao Tung University, Hsinchu 30050, Taiwan

Y. P. Lan and S. C. Wang

Institute of Electro-Optical Engineering, National Chiao Tung University, Hsinchu 30050, Taiwan

Received March 16, 2000

We demonstrate a compact and efficient diode-end-pumped TEM<sub>00</sub> laser with output power of 30 W for 48 W of incident pump power by use of two coated Nd:YVO<sub>4</sub> crystals to form a thermally stabilized flat-flat cavity. In *Q*-switched operation 25 W of average power at a pulse-repetition rate of 100 kHz and ~0.9-mJ pulse energy at a pulse-repetition rate of 10 kHz were produced. © 2000 Optical Society of America  
OCIS codes: 140.3480, 140.3540.

Although diode-end-pumped lasers are already available in commercial products employed in a variety of applications, scaling to higher power with good efficiency is still plagued by thermal aberrations and thermally induced fracture.<sup>1,2</sup> In particular, scaling to the 30-W level with 50% efficiency is difficult in diode-end-pumped Nd-doped lasers. Recently Nighan *et al.*<sup>3</sup> employed two Z building blocks with a cavity length of ~50 cm to generate 35 W of average power with a total of 56.5 W of pump power. Their laser system consisted of four fiber-coupled 20-W diode bars, two Nd:YVO<sub>4</sub> crystals, and six cavity mirrors.

Previously the thermal-lasing effect was integrated into a cavity design, resulting in a compact device with good beam quality and high efficiency.<sup>4,5</sup> In this Letter we demonstrate a compact and efficient diode-pumped laser with a cw TEM<sub>00</sub> output of 30 W by use of a symmetrical, thermally stabilized flat-flat cavity formed by two coated Nd:YVO<sub>4</sub> crystals. The performance of this laser in *Q*-switched operation is also reported.

Figure 1 is a schematic of the two-crystal laser cavity utilized in the experiment. The pump power consists of two 30-W fiber-coupled diode-laser arrays (FAP-81-30C-800-B) with the output wavelength of the lasers at 25 °C ranging from 807 to 810 nm. The fibers were drawn into round bundles of 0.8-mm diameter and a numerical aperture of 0.18. A focusing lens with 12.5-mm focal length and 87% coupling efficiency was used to reimage the pump beam into the laser crystal. The waist diameter of the pump beam was approximately 400 μm. The Nd<sup>3+</sup> concentration of the Nd:YVO<sub>4</sub> crystals was 0.3 at.%, and the length was 9 mm. Nd:YVO<sub>4</sub> crystals with low doping concentration were used to prevent thermally induced fracturing. Both laser crystals were *a* cut, which yielded a high-gain  $\pi$  transition. The Nd:YVO<sub>4</sub> crystal was wrapped with indium foil and mounted in a water-cooled copper block. The water temperature was maintained at 17 °C. One side of one Nd:YVO<sub>4</sub> crystal was coated to be nominally highly reflecting (HR) at 1064 nm ( $R > 99.9\%$ ) and highly transmitting (HT) at 808 nm ( $T > 95\%$ ). The other side was antireflecting at 1064 nm ( $R < 0.2\%$ ). One side of the other Nd:YVO<sub>4</sub> crystal was coated to be an output

coupler with 80% reflection at 1064 nm. The other side was also antireflecting at the laser wavelength ( $R < 0.2\%$ ). The 20-mm-long *Q* switcher (Gooch and Housego) had antireflection coatings at 1064 nm on both faces and was driven at a 40.7-MHz center frequency with 3.0 W of rf power.

The thermally induced lens in the laser crystal brings the flat-flat cavity into geometric stability. This concept was found at nearly the same time by Zayhowski and Mooradian<sup>6</sup> and by Dixon *et al.*<sup>7</sup> For a paraxial coherent beam propagating in the *z* direction over an infinitesimal distance *dz*, the differential optical path difference is given by<sup>8,9</sup>

$$\frac{d\varphi(r, z)}{dz} = \frac{\partial n}{\partial T} \Delta T(r, z) + (n - 1) \frac{\partial u(r, z)}{\partial z} + \sum_{i, j=1}^3 \frac{\partial n}{\partial \epsilon_{ij}} \epsilon_{ij}, \quad (1)$$

where the first term results from the thermal dispersion  $\partial n/\partial T$  and the steady-state temperature difference  $\Delta T(r, z)$ , the second term is caused by the thermally induced relative axial expansion  $\partial u(r, z)/\partial z$  of the crystal, and the third term represents the strain-induced birefringence with strain tensor  $\epsilon_{ij}$ . In most cases the contribution from thermal stress-induced birefringence is small. Note that the factor  $(n - 1)$  in Eq. (1) has to be replaced with  $n$  in the case of end-pumped resonators with a high-reflectivity coating on one end surface of the rod. This is required because for an internal reflection the total refractive index of the laser rod has to be taken into account. In the case of a conventional edge-cooled crystal with a top-hat pump intensity

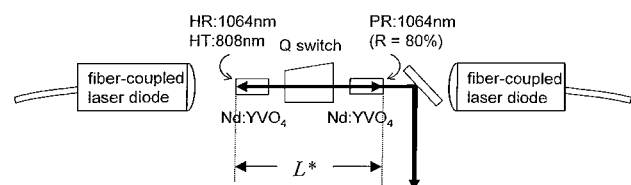


Fig. 1. Configuration of the diode-end-pumped Nd:YVO<sub>4</sub> laser.

profile, the steady-state temperature distribution is given by<sup>9,10</sup>

$$\begin{aligned} \Delta T(r, z) &= T(r, z) - T(r_b, z) \\ &= \frac{\xi P_{\text{abs}}}{4\pi K_c} \frac{\alpha}{1 - \exp(-\alpha l)} \\ &\quad \times \exp(-\alpha z) \left( \left[ 1 - \frac{r^2}{\omega_p^2(z)} \right] \right. \\ &\quad \left. + \ln \left[ \frac{r_b^2}{\omega_p^2(z)} \right] \right) \Theta[\omega_p^2(z) - r^2] \\ &\quad + \ln \left( \frac{r_b^2}{r^2} \right) \Theta[r^2 - \omega_p^2(z)], \end{aligned} \quad (2)$$

where  $\xi$  is the fractional thermal loading,  $K_c$  is the thermal conductivity,  $P_{\text{abs}}$  is the absorbed pump power,  $\alpha$  is the absorption coefficient at the pumping wavelength,  $l$  is the crystal length, and  $\omega_p(z)$  is the pump size in the active medium. Using the usual  $M^2$  propagation law, we find that the pump beam is given by

$$\omega_p^2(z) = \omega_{p0}^2 \left\{ 1 + \left[ \frac{\lambda_p M_p^2}{n\pi \omega_{p0}^2} (z - z_0) \right]^2 \right\}, \quad (3)$$

where  $\omega_{p0}$  is the radius at the waist,  $\lambda_p$  is the pump wavelength,  $M_p^2$  is the pump-beam quality factor, and  $z_0$  is focal plane of the pump beam in the active medium.

The inhomogeneous temperature distribution leads to stresses, strains, and displacement. The thermally induced strains for a nonuniformly heated solid can be solved from the equilibrium equation<sup>11</sup>

$$\frac{1 - \nu}{1 + \nu} \nabla(\nabla \cdot \mathbf{u}) - \frac{1 - 2\nu}{1 + \nu} \nabla \times \nabla \times \mathbf{u} = \alpha_T \nabla(T), \quad (4)$$

where  $\nu$  is the Poisson ratio,  $\alpha_T$  is the thermal-expansion coefficient, and  $\mathbf{u}$  is the displacement vector. A computer code that is part of the ANSYS thermal-analysis package was employed to find the numerical solution. The simulation results show that the magnitude of  $\partial u(r, z)/\partial z$  is 10–20% larger than  $\alpha_T \Delta T$  on average. Substituting the simulation result into Eq. (1) and carrying out the integration along the crystal axis, we then calculated the total optical path difference. Following the procedure of Ref. 8, we determined the focal length of the thermally induced lens,  $f_{\text{th}}$ , by fitting the calculated optical path difference with an equivalent spherical lens over the extent of the pump region with a least-squares fit.

Taking the thermal-lensing effect into account, we find the mode size at the input face of the laser crystal:

$$\omega_l = \left( \frac{\lambda f_{\text{th}}}{\pi} \sqrt{\frac{L}{2f_{\text{th}} - L}} \right)^{1/2}, \quad (5)$$

$$L = L^* + l \left[ \left( \frac{1}{n} \right) - 1 \right] + l_Q \left[ \left( \frac{1}{n_Q} \right) - 1 \right], \quad (6)$$

where  $L^*$  is the cavity length,  $l_{\text{KTP}}$  is the length of the KTP crystal,  $l_Q$  is the length of the Q-switched crystal,

and  $n_Q$  is the refractive index of the Q-switched crystal for the output laser beam. Equation (5) indicates that the mode size depends on the thermal lens and the effective cavity length.

An end-pump-induced thermal lens is not a perfect lens but rather an aberrated lens. It has been found that the thermally induced diffraction loss at a given pump power is a rapidly increasing function of mode-size–pump-size ratio. Practically, the trade-off between overlapping efficiency and thermally induced losses limits the mode-size–pump-size ratio to the range of approximately 0.6–1.0 when the incident pump power is greater than 5 W. The dependence of the mode-size–pump-size ratio on the pump power for the present cavity was calculated by use of Eqs. (5) and (6) and the following parameters:  $\xi = 0.24$ ,  $K_c = 0.0523$  W/K cm,  $\omega_{p0} = 0.2$  mm,  $M_p^2 \approx 310$ ,  $n = 2.165$ ,  $n_Q = 2.33$ ,  $l = 9$  mm,  $l_Q = 20$  mm,  $\nu = 0.28$ ,  $\partial n/\partial T = 3.0 \times 10^{-6}$ /K, and  $\alpha_T = 4.43 \times 10^{-6}$ /K. The calculation results for several cavity lengths are shown in Fig. 2. It is clear from Fig. 2 that the mode-size–pump-size ratio is approximately 0.7 at  $L^* = 80$ –90 mm for pump powers in the range 10–50 W, leading to a good compromise between overlapping efficiency and thermal effect.

Figure 3 shows the average output power in cw mode and Q-switched mode at a repetition rate of 100 kHz as a function of the absorbed pump power. The output power in cw mode was measured before insertion of the Q switch into the resonator. The highest output power of 30 W was achieved at the absorbed pump power of 48 W. The average slope efficiency with respect to the absorbed pump power was 66.6%. To our knowledge these are the highest efficiency and power ever reported for a thermally stabilized flat–flat cavity. The  $M^2$  parameter was measured to be  $<1.5$  over the complete output power range. Recently a composite crystal structure,<sup>1</sup> which was fabricated by diffusion bonding of a doped crystal to an undoped piece of the same cross section, was used to reduce thermally induced stress. We believe

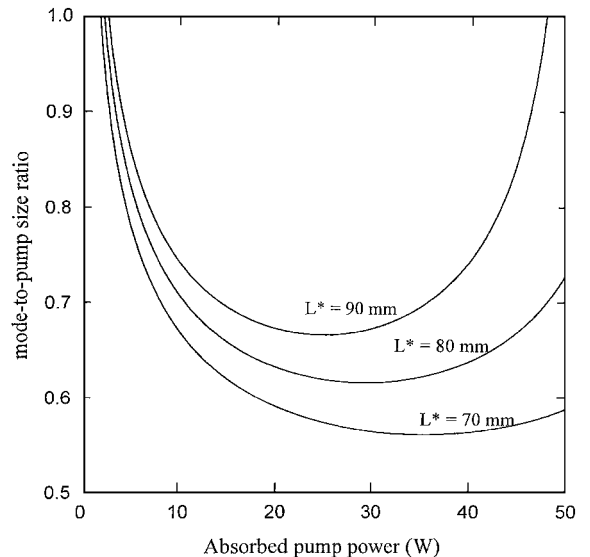


Fig. 2. Dependence of the mode-size–pump-size ratio on the absorbed pump power for several cavity lengths.

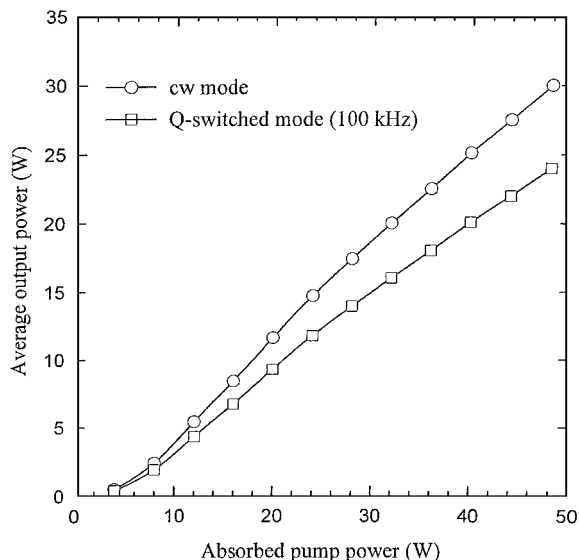


Fig. 3. Average green output power as a function of the absorbed pump power.

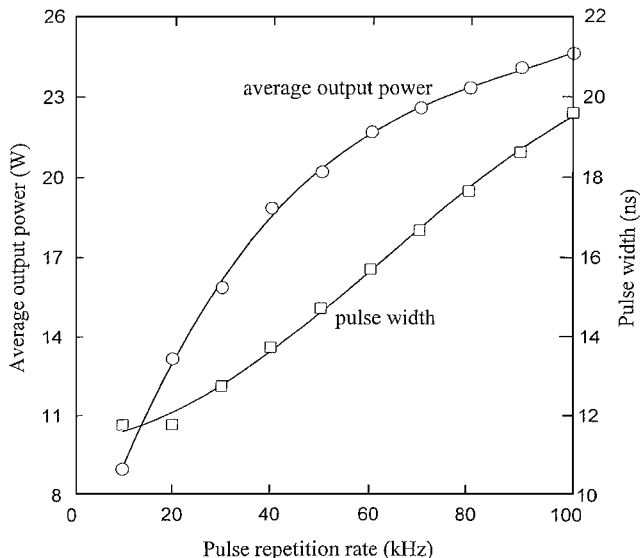


Fig. 4. Average green output power and pulse width as functions of  $Q$ -switched pulse-repetition frequency at a pump power of 48 W.

that higher output power with better beam quality can be achieved with a composite crystal structure. With the  $Q$  switch in the cavity, stable  $Q$ -switched mode operation at a pulse-repetition rate of up to 100 kHz was accomplished. As shown in Fig. 3, the highest average output power obtained at a 100-kHz pulse-repetition rate was 25 W at a pump power of 48 W.

Figure 4 shows the average output power and pulse width at a pump power of 48 W as a function of the pulse-repetition rate. To avoid damage to the intracavity optical components we operated the repetition rate at greater than 10 kHz. It can be seen from Fig. 4 that at low pulse-repetition rates the pulse width is short and the energy per pulse

is high, whereas at higher pulse-repetition rates the energy per pulse is low and the pulse width is long but the average power is high. The highest  $Q$ -switched pulse energy of 0.9 mJ was achieved at 10 kHz. At less than 10 kHz, no further increase of the pulse energy was observable, owing to the 90–100- $\mu$ s lifetime of the upper laser level of the Nd:YVO<sub>4</sub> crystal. The major advantage of the Nd:YVO<sub>4</sub> crystal is its ability to retain a short pulse width even at very high pulse-repetition rates. At full pump power the pulse width varies from 12 ns at 10 kHz to 20 ns at 100 kHz. With a Nd:YAG crystal in the present cavity, the pulse width increases from 20 ns at 10 kHz to 50 ns at 100 kHz. The pulse width in the Nd:YVO<sub>4</sub> crystal is approximately 2–3 times shorter than that in Nd:YAG, owing to the shorter lifetime in the Nd:YVO<sub>4</sub> crystal. For high pulse-repetition rates (>30 kHz), the output performance of the Nd:YVO<sub>4</sub> system is generally better than that of the Nd:YAG or the Nd:YLF system, owing to higher optical-to-optical conversion efficiency.

We have demonstrated the use of a thermal lens to obtain a highly efficient, high-power solid-state laser in cw and  $Q$ -switched modes. The laser cavity was directly formed by two coated 0.3-at. % Nd:YVO<sub>4</sub> crystals. An YVO<sub>4</sub> crystal of low Nd concentration was used to avoid thermally induced fracture. With the thermally induced lensing effect, the cavity length was adjusted to yield the optimal mode-size matching for the maximum output power. 30 W of TEM<sub>00</sub> cw mode output power with good beam quality was obtained at 48-W pump power. In  $Q$ -switched operation, we demonstrated the potential of the YVO<sub>4</sub> crystal to generate pulse energy in the millijoule range with high pulse-repetition rates. Such a laser source will be interesting for micromaterials processing applications.

## References

1. M. Tsunekane, N. Taguchi, T. Kasamatsu, and H. Inaba, *IEEE J. Sel. Top. Quantum Electron.* **3**, 9 (1997).
2. L. Gonzalez, K. Kleine, and L. R. Marshall, in *Conference on Lasers and Electro-Optics, 1999 OSA Technical Digest Series* (Optical Society of America, Washington, D.C., 1999), p. 1.
3. W. L. Nighan, Jr., N. Hodgson, E. Cheng, and D. Dudley, in *Conference on Lasers and Electro-Optics, 1999 OSA Technical Digest Series* (Optical Society of America, Washington, D.C., 1999), p. 1.
4. Y. F. Chen, *Opt. Lett.* **24**, 1032 (1999).
5. Y. F. Chen, *IEEE Photon. Technol. Lett.* **9**, 669 (1998).
6. J. J. Zayhowski and A. Mooradian, *Opt. Lett.* **14**, 1989 (1989).
7. G. J. Dixon, L. S. Lingvay, and R. H. Jarman, *Proc. SPIE* **1104**, 107 (1989).
8. C. Pfistner, R. Weber, and H. P. Weber, *IEEE J. Quantum Electron.* **30**, 1605 (1994).
9. A. K. Cousins, *IEEE J. Quantum Electron.* **28**, 1057 (1992).
10. A. K. Cousins, *Appl. Opt.* **31**, 7259 (1992).
11. L. D. Landau and E. M. Lifshitz, *Theory of Elasticity* (Pergamon, New York, 1986), p. 16.